REPORT DOCUMENTATION PAGE

Form Approved
OMB No. 0704-0188

Public reporting burden for this collection of information is estimated to average 1 hour per response, including the time for reviewing instructions, searching existing data sources, gathering and maintaining the data needed, and completing and reviewing this collection of information. Send comments regarding this burden estimate or any other aspect of this collection of information, including suggestions for reducing this burden to Department of Defense, Washington Headquarters Services, Directorate for Information Operations and Reports (0704-0188), 1215 Jefferson Davis Highway, Suite 1204, Arlington, VA 22202-4302. Respondents should be aware that notwithstanding any other provision of law, no person shall be subject to any penalty for failing to comply with a collection of information if it does not display a currently valid OMB control number. **PLEASE DO NOT RETURN YOUR FORM TO THE ABOVE ADDRESS.**

1. REPORT DATE *(DD-MM-YYYY)*	**2. REPORT TYPE**	**3. DATES COVERED** *(From - To)*
June 2013	Technical Paper	June 2013-July 2013

4. TITLE AND SUBTITLE
Computational and Experimental Investigation of Transverse Combustion Instabilities

5a. CONTRACT NUMBER

5b. GRANT NUMBER

5c. PROGRAM ELEMENT NUMBER

6. AUTHOR(S)
Park. K., Sardeshmukh, S., Heister, S. and Sankaran, V.

5d. PROJECT NUMBER

5e. TASK NUMBER

5f. WORK UNIT NUMBER
Q12M

7. PERFORMING ORGANIZATION NAME(S) AND ADDRESS(ES)

Air Force Research Laboratory (AFMC)
AFRL/RQR
5 Pollux Drive
Edwards AFB CA 93524-7048

8. PERFORMING ORGANIZATION REPORT NO.

9. SPONSORING / MONITORING AGENCY NAME(S) AND ADDRESS(ES)
Air Force Research Laboratory (AFMC)
AFRL/RQR
5 Pollux Drive
Edwards AFB CA 93524-7048

10. SPONSOR/MONITOR'S ACRONYM(S)

11. SPONSOR/MONITOR'S REPORT NUMBER(S)
AFRL-RQ-ED-TP-2013-169

12. DISTRIBUTION / AVAILABILITY STATEMENT
Distribution A: Approved for Public Release; Distribution Unlimited. PA#13433

13. SUPPLEMENTARY NOTES
Conference paper for the 49th AIAA/ASME/SAE/ASEE Joint Propulsion Conference, San Jose, CA, 15-17 July 2013.

14. ABSTRACT

Concurrent experiments and computations are used to analyze combustion instabilities in a transverse mode combustion chamber. The experiments employ a shear-coaxial injector element, positioned within a rectangular chamber. The reacting flow portion of the study element is optically accessible and the chamber is extensively instrumented with high-frequency pressure transducers. High amplitude transverse acoustics modes are driven by unstable injector elements located near the chamber end-walls. Different levels of instability are obtained by varying the operation of these driving elements. High-fidelity computational fluid dynamics simulations are used to model this set-up, although only the study element is fully represented and the transverse acoustics modes are generated by vibrating the side walls at the appropriate frequencies. The computational results are compared quantitatively with the high frequency pressure measurements, and qualitatively by using the CH* chemiluminescence signal from the experiment. The combustion response of the first, second and third transverse modes obtained using a dynamic modal decomposition procedure show excellent agreement between the experiments and simulations. The overall approach shows significant promise for screening the combustion response of candidate injector configurations for rocket applications.

15. SUBJECT TERMS

16. SECURITY CLASSIFICATION OF:			**17. LIMITATION OF ABSTRACT**	**18. NUMBER OF PAGES**	**19a. NAME OF RESPONSIBLE PERSON**
					Venkateswaran Sankaran
a. REPORT	**b. ABSTRACT**	**c. THIS PAGE**	SAR	14	**19b. TELEPHONE NO** *(include area code)*
Unclassified	**Unclassified**	**Unclassified**			661-525-5534

Standard Form 298 (Rev. 8-98)
Prescribed by ANSI Std. 239.18

Computational and Experimental Investigation of Transverse Combustion Instabilities

Kevin Shipley[1], Collin Morgan[2], William E. Anderson[3]
Purdue University, West Lafayette, IN, 47906

and

Matthew E. Harvazinski[4], Venkateswaran Sankaran[5]
Air Force Research Laboratory, Edwards AFB, CA, 93524

Concurrent experiments and computations are used to analyze combustion instabilities in a transverse mode combustion chamber. The experiments employ a shear-coaxial injector element, positioned within a rectangular chamber. The reacting flow portion of the study element is optically accessible and the chamber is extensively instrumented with high-frequency pressure transducers. High amplitude transverse acoustics modes are driven by unstable injector elements located near the chamber end-walls. Different levels of instability are obtained by varying the operation of these driving elements. High-fidelity computational fluid dynamics simulations are used to model this set-up, although only the study element is fully represented and the transverse acoustics modes are generated by vibrating the side walls at the appropriate frequencies. The computational results are compared quantitatively with the high frequency pressure measurements, and qualitatively by using the CH* chemiluminescence signal from the experiment. The combustion response of the first, second and third transverse modes obtained using a dynamic modal decomposition procedure show excellent agreement between the experiments and simulations. The overall approach shows significant promise for screening the combustion response of candidate injector configurations for rocket applications.

I. Introduction

COMBUSTION instability occurs due to the coupling between the combustion heat release and the acoustic modes of a combustor and is one of the most challenging problems in rocket engine development. At high amplitudes the instability has the power to destroy an engine through vibration and increased heat release. Due to the nonlinearity of the combustion processes and low acoustic damping, extremely high rates of heat addition, and the multiple scales and processes that can participate, combustion instability is difficult to predict. Small changes in geometry or operating conditions can result in an unstable system [1, 2].

One approach to developing a full-sized rocket engine is to use subscale testing with the goal being to simulate the performance, stability, heat transfer, and ignition of a full-scale device in a smaller apparatus. Through subscale testing, greater flexibility can be introduced in the development process since design changes can be investigated more quickly and with less expense. The difficulty with subscale testing is replicating the physical and chemical processes of the full-scale environment in the subscale engine. The conflicting requirements of the two sizes make it impossible to match all processes exactly [3]. This is particularly problematic for high-frequency combustion stability phenomena since the chamber acoustic modes are determined by the chamber dimensions. Nevertheless, subscale testing can provide a useful means of collecting data for validating computational fluid dynamics (CFD) models that can subsequently be applied to full-scale configurations to help assess scale-up issues. Moreover, CFD is instrumental in shedding light on the fundamental physical and chemical processes underlying combustion stability, as well as providing a basis for combustion response functions for use in engineering stability models.

[1] Graduate Research Assistant, School of Aeronautics and Astronautics and Member AIAA.
[2] Graduate Research Assistant, School of Aeronautics and Astronautics and Student Member AIAA.
[3] Professor, School of Aeronautics and Astronautics and Associate Fellow AIAA.
[4] Scientist, Rocket Propulsion Division and Member AIAA.
[5] Senior Scientist, Rocket Propulsion Division and Senior Member AIAA.

Distribution Statement A: Approved for public release; distribution is unlimited.

The results presented here are part of a long-term effort to develop a hierarchy of experiments, analysis, and simulations that can be combined to produce accurate and reliable predictions of combustion dynamics in full-scale systems. As part of that effort, a subscale rectangular chamber has been developed to replicate oscillating flowfields that are the dominating features of transverse instabilities. A "study element" is placed in the chamber, and its response to oscillations at varying levels of amplitude is determined, for example by measuring the light emission of combustion. Concurrently, a hybrid RANS/LES model is applied to model the experimental set-up and the results are compared with the measured data. In addition to validation, the simulations can also provide useful insight into the physics of combustion dynamics and its coupling with the chamber acoustics. Moreover, the computational model can be applied to other conditions and geometries and provide a design and analysis capability to guide new rocket engine development.

The experimental combustor contains seven injector elements, of which the central element is the study element whose combustion response is being evaluated. The remaining six are "driving" elements that are arranged three on each side of the study element and are tuned so that they drive transverse mode instabilities in the rectangular chamber. The amplitude of the transverse oscillations can be controlled by varying the operation of the driving elements. The set-up allows us to estimate the combustion response of the study element. Specifically, the chamber is instrumented by several high-frequency pressure transducers mounted on the walls of the chamber. In addition, the reacting flow region corresponding to the study element is out-fitted with a window in order to provide optical access for measurements of CH* chemiluminescence.

Companion computational simulations of the experimental set-up are also performed in this study. Because a full simulation of all the seven injectors would be computationally expensive, only the study element and the one of the elements on either side of the study element are included in the simulation. The outer two elements near the end walls of the combustor, which drive the oscillations, are replaced by an in-flow boundary condition representing the combustion products being supplied by these injector elements. In the simulations, the transverse oscillations in the chamber are driven by an oscillating velocity component at the side-walls of the chamber. The objectives of the present study are two-fold: (1) to demonstrate the ability of the experimental apparatus to evaluate the combustion response of the study element, and (2) to establish a modeling framework that can be used to predict the combustion response, shed insight into the underlying physical mechanism and, eventually, to provide a design and analysis capability of relevance to rocket engine development.

The outline of the paper is as follows. First, an overview of the experimental combustor that can generate varying amplitudes of transverse oscillations is provided along with some sample results. Following this, a description of the three-dimensional hybrid RANS/LES code used to simulate the experiment is given. Computational results where the end-wall velocity is oscillated to produce transverse pressure and velocity oscillations are compared to the experimental wall-pressure measurements. The results show that the approach can produce reasonably good approximations of the measured unsteady flowfield. Further, simulations of the reacting flowfield corresponding to the study element are presented, and compared with the chemiluminescence signal obtained in the experiments. Comparisons are made on the basis of results from a modal decomposition analysis at frequencies corresponding to the first through the third transverse chamber modes.

II. Experimental Setup and Measurements

The transverse instability combustor (TIC) experimental apparatus is shown in Figure 1. The TIC was developed at Purdue University to analyze combustion response to high amplitude velocity oscillations commonly associated with transverse combustion instability [4]. The combustor has a linear array of seven injector elements through which fuel and oxidizer flow into a windowed chamber. A nozzle is affixed to the aft-end of the chamber. The center injector is the study element and the three injectors on either side are the so-called driving elements. The driving elements are gas-centered swirl coaxial injectors and produce varying levels of pressure fluctuations ranging from 8% to 65% of the mean chamber pressure. The amplitude of the oscillations is controlled by selecting which of these elements flow bipropellant (fuel and oxidizer) and which ones flow only the oxidizer. In this study, the fuel used in the driving elements is RP1 and ethane is used for the study element. The oxidizer is decomposed hydrogen peroxide for all elements.

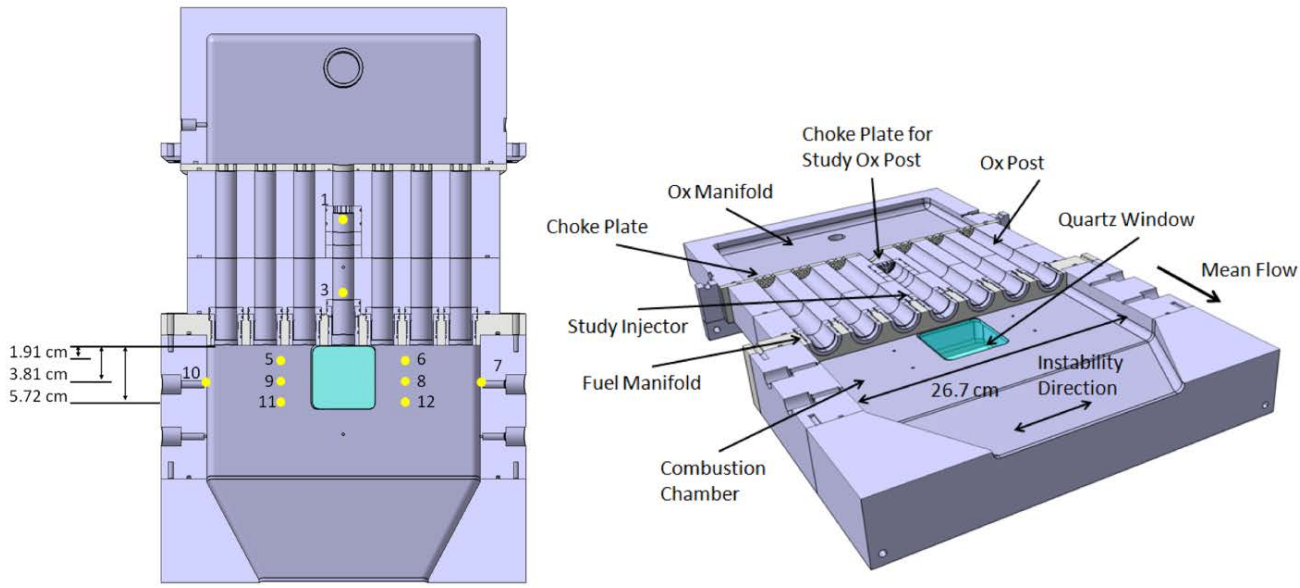

Figure 1: Transverse instability combustor, yellow dots indicate the location of high-frequency pressure transducers.

Table 1 shows the observed pressure amplitudes and frequency for four different injector configurations. O represents bipropellant flow and X represents oxidizer-only flow through the injector. The first configuration gives the maximum chamber pressure (P_c) and the highest pressure fluctuations (P'), while the third configuration gives the lowest fluctuations.

Table 1: Instability configuration.

No.	Configuration	P_c [kPa]	P' [kPa]	P', % P_c	1W Freq [Hz]
1	OOXOXOO	965	620	65%	2032
2	OXXOXXO	830	415	50%	1807
3	XOXOXOX	815	70	8%	1855
4	XOOOOOX	895	175	20%	1920

The combustor is instrumented with ten high-frequency pressure transducers to record the fluctuations in chamber pressure. The locations of the transducers are marked in Figure 1. Transducers 7 and 10 are located on the chamber wall where there is a pressure antinode for the 1W mode. Two transducers are located in the study element oxidizer post and the remaining six are located on either side the chamber window. Two low-frequency transducers are used at the base of the chamber to measure the mean pressure.

To measure the combustion response of the study element, CH* chemiluminescent images are captured at a framing rate of 20,000 fps through the chamber window. A more detailed description is given in Ref. 9. The images provide a qualitative measurement of the combustion heat release showing varying regions of intensity where the combustion is taking place. When analyzed in combination with the high-frequency pressure measurements, they can provide a semi-quantitative measurement of the combustion response, as well as physical insight into how the reacting flow of the study element interacts with the oscillating flowfield.

III. Computational Setup and Measurements

A. Computational Model

An in-house CFD code called the General Equation and Mesh Solver, GEMS is used for the simulations [5-8]. GEMS uses a second-order finite-volume approach to solve the Navier-Stokes equations along with continuity, energy and six coupled species equations. A duel-time approach is used to eliminate approximate factorization errors. To account for turbulence, a hybrid RANS/LES model is used with a two-equation k-ω model near the wall.

Combustion is modeled using a two-step global reaction incorporating five species. The species are chosen based on a chemical equilibrium analysis of ethane combustion. Global reactions allow the coupling of unsteady heat release and pressure to be captured while minimizing the number of species that must be included. An equilibrium reaction is used to predict the concentrations of CO, CO_2, and O_2.

$$\mathbf{C_2H_6} + \frac{\mathbf{5}}{\mathbf{2}}\mathbf{O_2} \Rightarrow \mathbf{2CO} + \mathbf{3H_2O} \qquad \text{(Eq. 1)}$$

$$\mathbf{CO} + \frac{\mathbf{1}}{\mathbf{2}}\mathbf{O_2} \Leftrightarrow \mathbf{CO_2} \qquad \text{(Eq. 2)}$$

The reaction rates of Eqs. 1 and 2 use a modified Arrhenius function whose coefficients are chosen to match the laminar flame speed [11].

The seven injector array used in the experimental set-up is expensive to simulate fully because of the large number of grid points required to resolve each injector. Instead, we use a reduced model, where only the study element and the injectors on either side of it are fully resolved. A schematic of the computational domain is shown in Figure 2. The additional driving injectors on either side of the central injector elements are replaced by uniform mass flow inlets. The inlet of the study element is a series of choked concentric slots and a constant mass flow is specified upstream of the slots. Decomposed hydrogen peroxide, (42% O_2 and 58% H_2O) at 1029 K flows through the study element as well as the two driving elements on either side. Ethane is injected through a fuel slot at the base of the study element at a temperature of 319 K. The operating conditions are set to match those of the experimental configuration 1 (Table 1). Thus, the driving injectors on either side of the central study-element flow only oxidizer while the incoming flow in the remaining driving injectors consists of combustion products - O_2, H_2O, CO and CO_2 - at 2600K. A further simplification is the introduction of oscillating side walls which are described in the following section. A back pressure of 101.325 kPa is specified at the nozzle exit. All walls are no-slip adiabatic walls with the exception of the driving walls. The computational mesh contains about 2.7 million grid points.

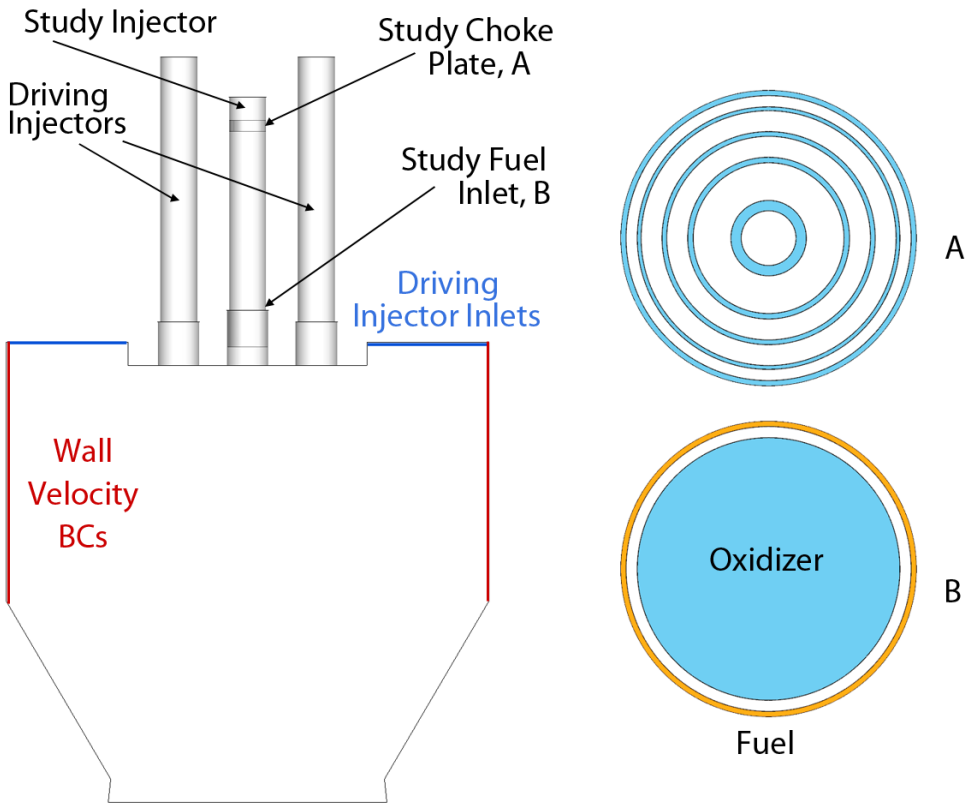

Figure 2: Computational domain for the simulation.

B. Oscillating Wall Boundary Condition

To generate the pressure oscillations in the combustor, the side walls (shown in Figure 2) are oscillated with a prescribed velocity according to,

$$w = A\sin(2\pi f + \varphi)$$

where w is the wall normal velocity, A, f, and φ are the specified amplitude, frequency and phase shift. The frequency is set to the primary acoustic frequency of the chamber obtained from the experimental results. The amplitude of the oscillations is modified to control the amplitude of the pressure fluctuations in the chamber. The velocity oscillations at the two walls are set in phase (φ = 0°) in order to generate the 1W instability. Figure 3 shows the amplitude of the 1W pressure fluctuations in the combustor for several wall velocities. The relationship is approximately linear and allows for a tuning of the pressure fluctuations in the CFD model to match the experiment. These results are obtained for a reacting flowfield in the chamber.

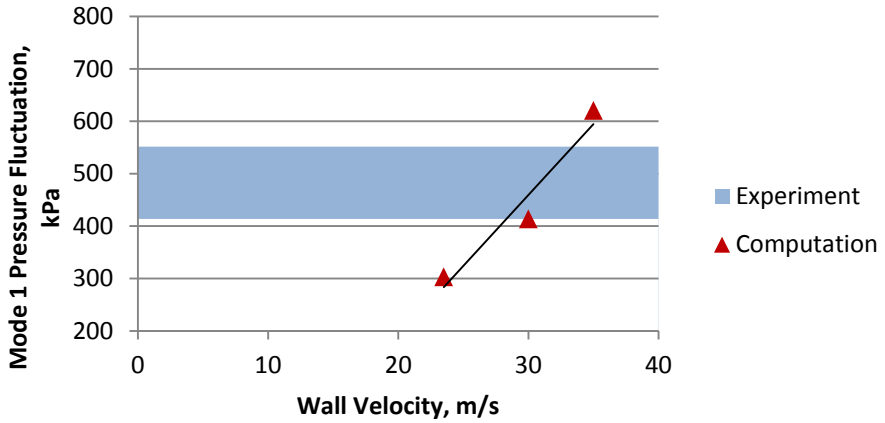

Figure 3: Effect of wall velocity on pressure.

The effect of the oscillating boundary on the pressure mode shapes is shown in Figure 4 for three different wall velocities. The pressure mode shape is a phase-averaged representation of the pressure in the combustion chamber. In the figure, the first and second acoustic modes are shown. These are obtained by filtering the data at the frequency of the primary and secondary acoustic modes. The dots shown on the plots represent the experimental data at ports 7, 8, 9 and 10. The results show that the primary pressure fluctuation amplitudes can be well matched with the experimental amplitude when the wall velocity is set to 30 m/s. Increasing the wall velocity amplitude also affects the higher harmonic modes as seen by the increase in the pressure mode shape amplitude filtered at the 2nd mode. While the primary mode seems well-matched, there is still a discrepancy in the second mode. Nevertheless, this is a good first-order approximation of the instability levels observed in the experiment. We note that better matches of all the modal amplitudes can be achieved by superimposing multiple frequencies of wall oscillation.

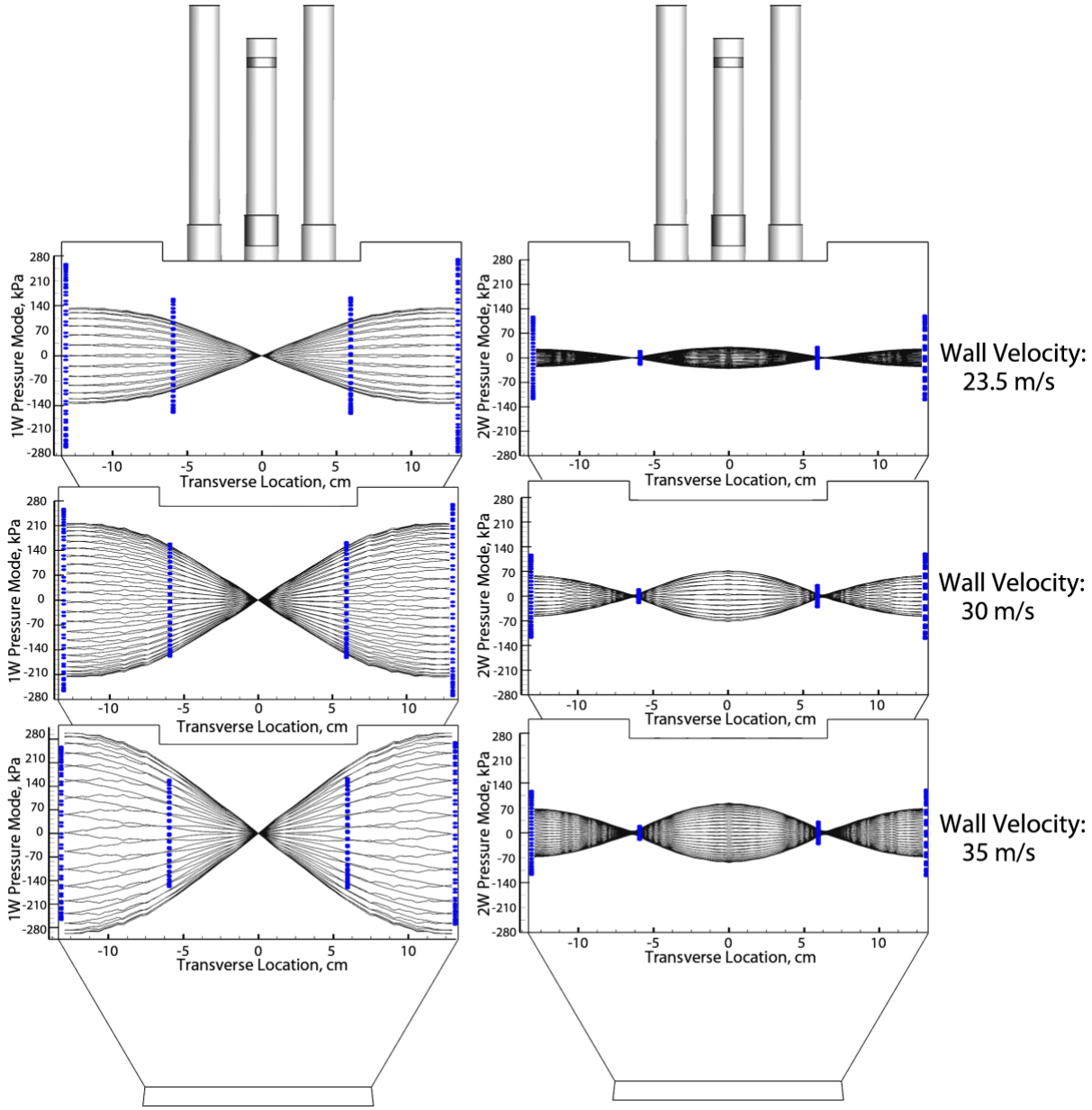

Figure 4: Pressure mode shapes for the 1st (left column) and 2nd (right column) modes. Each row represents a different wall velocity boundary condition: 23.5m/s (top), 30 m/s (middle), 35 m/s (bottom), experimental data from port 7 – 10 is overlaid in blue.

IV. Results

All computations are initialized using stationary walls in order to minimize the initial transient time of the simulation. At the start of the simulation, oxidizer flows through the three injectors and fuel is injected at the study fuel inlet. Bypass flow comprised of hot combustion products also begins to flow enter the domain through the driving inlets. The simulation with stationary walls after 4 ms is shown in Figure 5. Each frame shows a slice taken at the center of the combustor and is representative of the flowfield. The top row shows the ethane mass fraction, oxygen mass fraction and heat release contours. In the heat release contours, we can observe that the reacting flowfield in the center study element is flanked by reactions occurring between the CO and O_2 from the driving inlet. A zoomed-in view of the near-injector region is shown in the second row. The ethane burns quickly in the oxygen-rich environment and interacts with the oxygen from both the central study element and the adjacent oxidizer-only injectors.

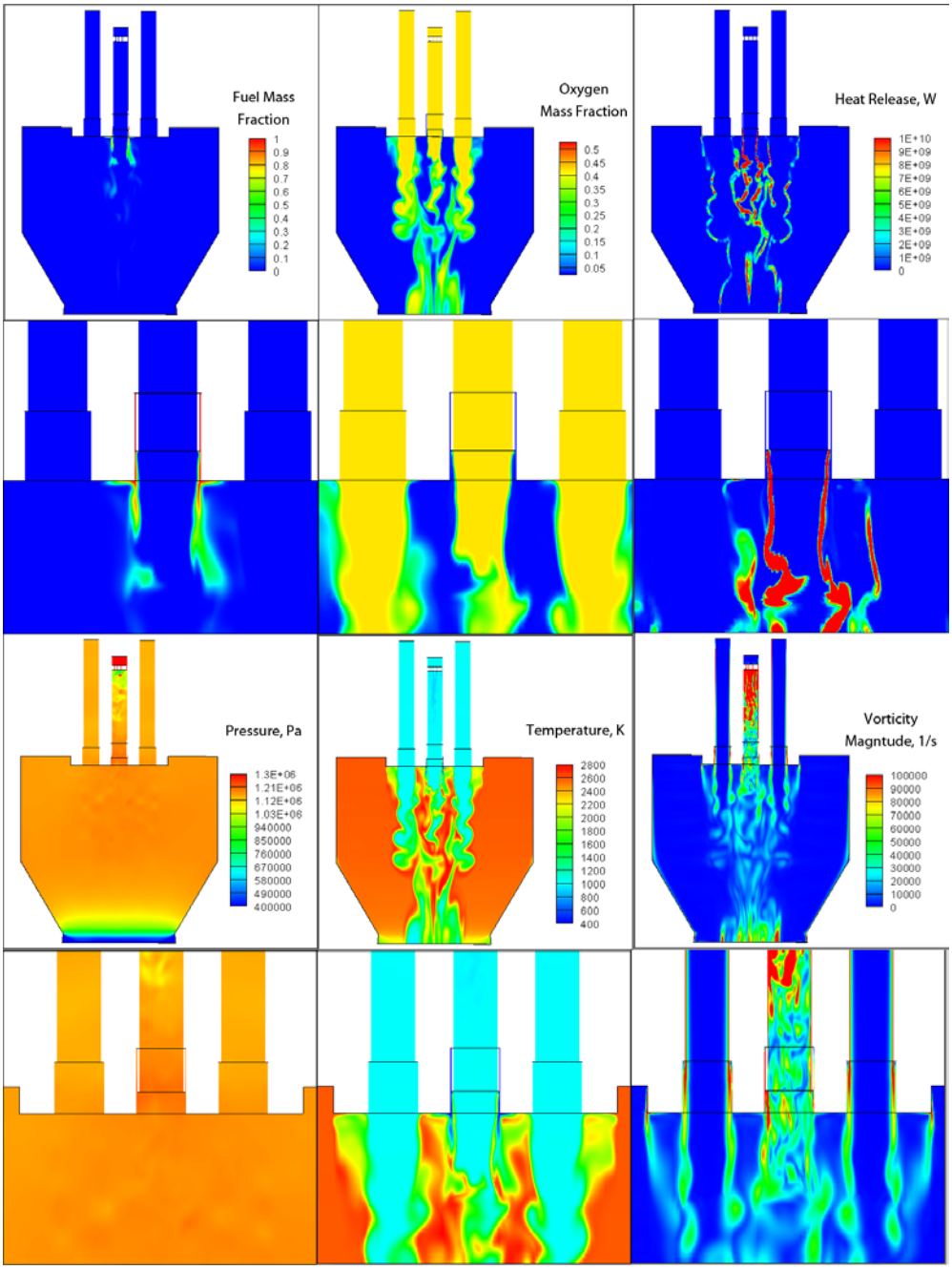

Figure 5: Chamber flowfield. The top row shows ethane mass fraction (left), oxygen mass fraction (middle) and heat release (right). The second row shows a zoomed-in view near the injection plane of the top row field. The third row shows pressure (left), temperature (middle) and vorticity (right). The bottom row shows a zoomed-in view near the injection plane of the third row field.

The third row shows the pressure, temperature and vorticity contours in the combustor. Pressure is uniform in the main chamber and oxidizer injectors, with the highest pressure occurring upstream of the study element choke-plate. The highest temperatures are seen in the central reacting region and by the side walls, which corresponds to combustion products. Vorticity is observed to be the highest downstream of the choke-plate, which is due to the vortex shedding that occurs in the region of the choked slots. Additional vortices are produced by the vortex shedding at the fuel injection lip, which is the region where the fuel and oxidizer first mix. A small amount of vorticity is also visible at the lips of the oxidizer-only driving injectors.

Once the flowfield has reached a near-stationary condition the side walls are oscillated to generate the high-amplitude 1W transverse mode in the chamber. The resulting pressure fluctuations in the chamber reach a limit cycle, beyond which the simulation is run for an additional 45 ms to produce sufficient data for analysis. The results of the simulation run with a specified wall velocity amplitude of 30 m/s is shown in Figure 6. The figure shows the pressure, temperature and heat release. The slices shown are located at the center of the chamber and each row represents a complete cycle defined as the pressure moving from left to right and then back. Each column of figures is at the same moment in time. At time-slice 1, the wavefront is at the right injector post and is moving from left to right. As the wave-front passes each injector, secondary compression waves are seen to move upstream into the injectors and are eventually reflected back into the chamber. The oxidizer injectors are designed so that the reflected wave re-enters the chamber as the transverse wave passes, which in turn helps drive the instability. Across the transverse wave there is also an increase in the temperature. When the wave reaches the right wall (time-slice 2), it reflects back to the left due to the wall boundary condition. The wave then passes through the center of the chamber, which disrupts the heat release. Once the wave hits the left wall it is reflected back to the right and the cycle repeats. The heat release disruption can clearly be seen in slices 4 and 5 with the wave moving from left to right. Once the wave finishes passing through the center there is an increase in heat release before the wave is reflected back.

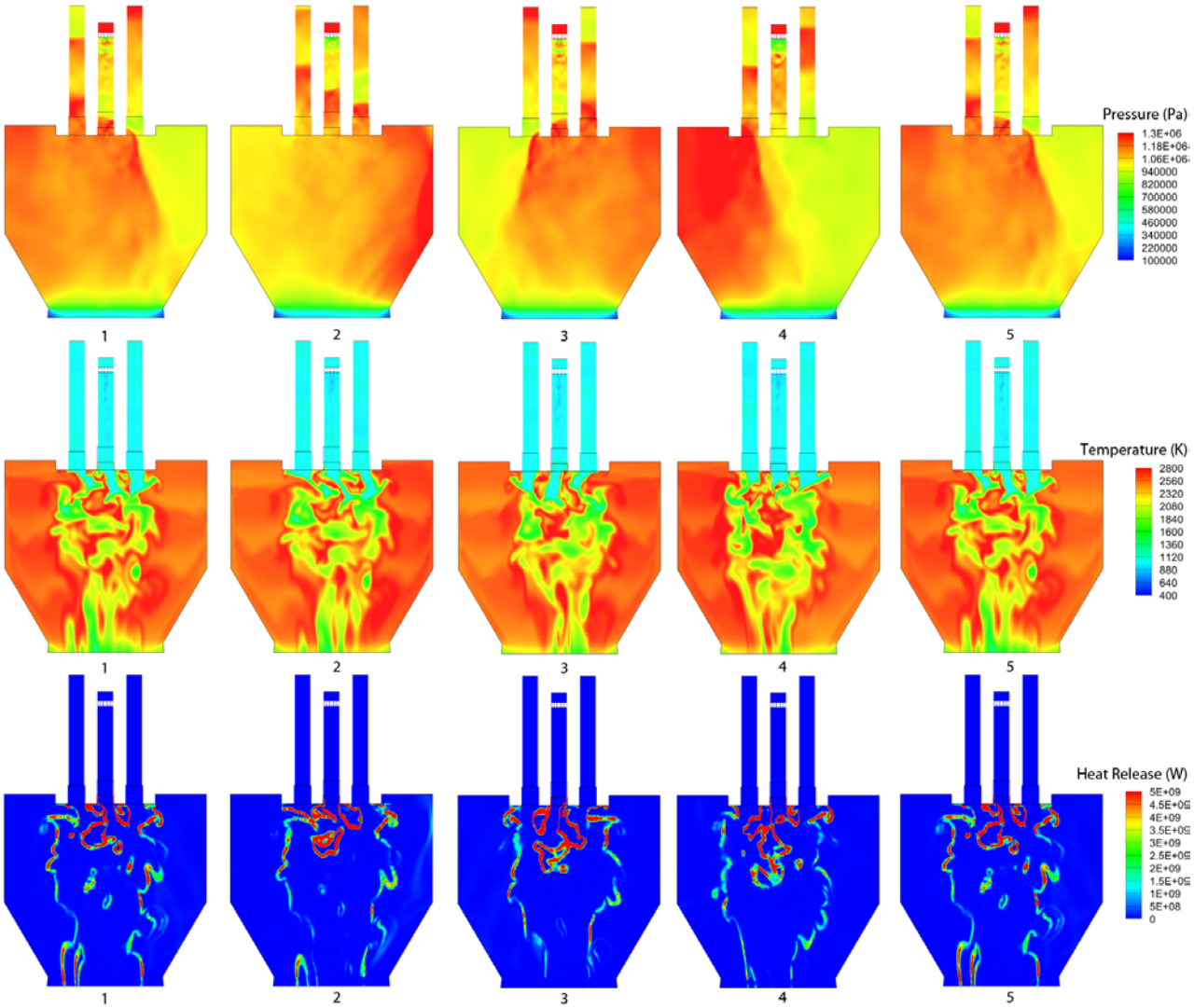

Figure 6: Simulation slices of pressure (top row), temperature (middle row), and heat release (bottom row).

The frequency content of the predicted results is analyzed and compared with the experimental measurements. The location used for the comparison is the pressure antinode on the wall (port 7). The results of a power spectral density (PSD) analysis of the data are shown in Figure 7. The analysis used 50 ms of data providing a frequency resolution of 20 Hz. The frequencies of the first mode for the experiment and simulation match very well. We note that this is expected since the first mode frequency is used as an input to the wall oscillation in the simulations. The second and third modes also match very well. The frequencies observed in the PSD can then used to filter the pressure signals and develop the mode shapes such as those shown in Figure 4. The pressure mode shape confirms that, by oscillating the wall velocity function at the experimental first mode frequency, the harmonics are also well captured.

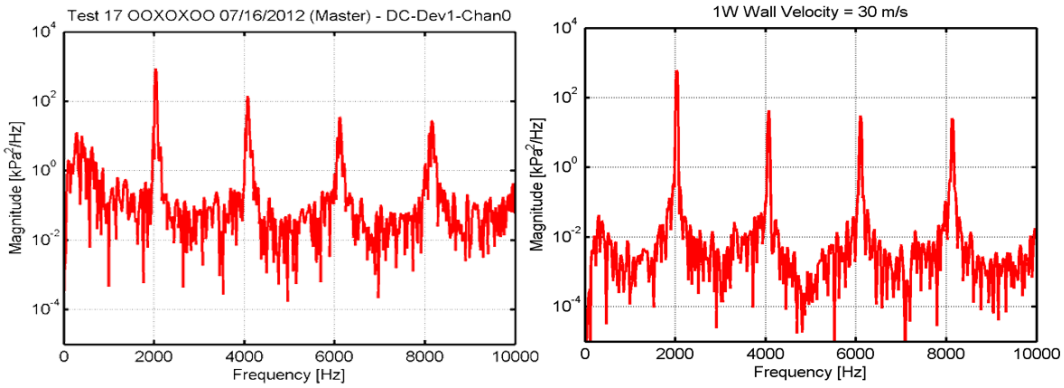

Figure 7: PSD Comparison between the experiment (left) and simulation (right).

A plot of the high-pass filtered pressure at 150 hz for ports 7-10 in the experiment and simulation is shown in Figure 8. The pressure at each port is plotted as a function of time. The travelling compression wave can be seen by examining the peaks in the pressure data. At point 1 the compression wave is at the left wall and is travelling to the right. When the wave reaches the left side of the window there is a peak in pressure seen by point 2. The wave is then dampened across the window at point 3. As the wave reaches the right wall energy is added to the wave by the side wall driving element, which is illustrated by point 4. The wave then reflects to the left and travels back across the chamber.

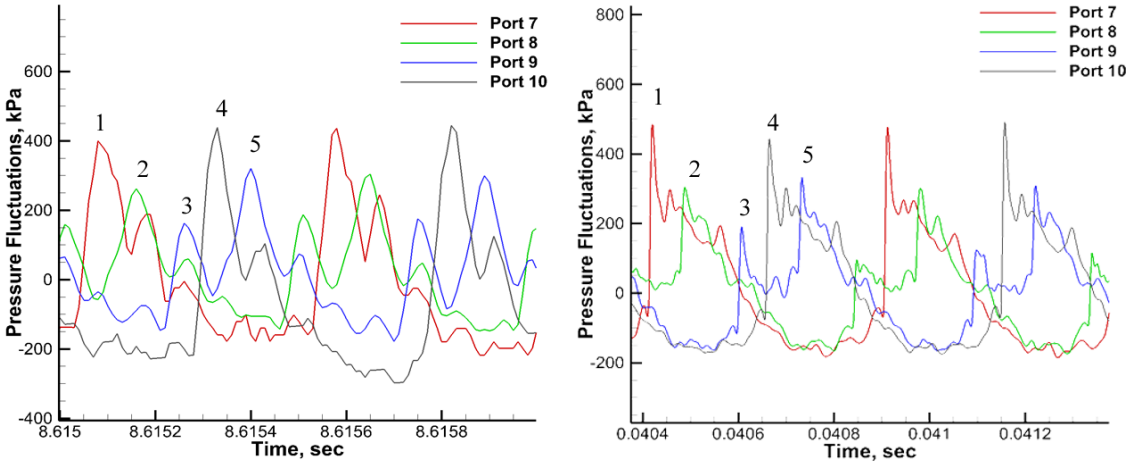

Figure 8: Pressure waveform comparison between the experiment (left) and simulation (right).

The pressure amplitudes are in good agreement between the simulation and experiment however there are a few differences in the waveform. The experimental waveforms at the walls all have a primary peak followed by a smaller secondary peak. The simulation however shows a primary peak, which is much sharper, followed by a second peak visible between points 1 and 2 and then a third peak at the end before the pressure drops off. The extra peak is due to a reflected wave from the inside driving injector wall boundary. A further difference is that when the

wave reaches a new port there is a higher discrepancy between the pressure at that port and the previous port location. This could suggest a more diffusive pressure wave in the simulation.

Images of the chemiluminescence from CH* taken in the experiment are compared with the combustion heat release from the simulation using a dynamic modal decomposition (DMD) procedure. This technique takes spatio-temporal data for the whole field and generates a frequency based modal representation. The CH* images and the CFD heat release fields are shown in Figure 9 for the first three modes. Those modes correspond to the first three peaks in Figure 7. Flow direction is from top to bottom and the transverse wave travels from side to side. The first row and third row represent the same geometric region in the simulations and experiments. The second row is a zoomed-in view of the first row to aid in the comparisons.

It is important to note that the experimental images are line of sight measurements, whereas the CFD images are slices at the center of the chamber. Given that, we observe that the mode shapes of the simulations are quite similar to those obtained in the experimental measurements of light emission, suggesting that the simulation is properly capturing the physics of the coupling between heat release and the oscillations. Our future plans include the ability to integrate the simulated heat release to permit a quantitative direct comparison.

In the center of the rectangular chamber where the study element is located, the 1W mode of the rectangular chamber produces a velocity antinode and a pressure node. The dominant effect of the oscillating transverse velocity can clearly be seen in the Mode 1 images in Figure 9. Both experiment and simulation show lobes of heat release with a plane of symmetry about the centerline of the study element. The heat release is a maximum on the leeward (downwind) side of the jet, suggesting that increased mixing occurs when the low-density oxidizer is pushed into the high-density fuel. On the windward side, the oxidizer is pushed away from the fuel, leading to a relative deficit in heat release. On the other hand, a pressure antinode is coincident with the study element for the second mode 2, and the 2W pressure oscillation does not produce a gradient of heat release across the study element. The slight differences that can be seen near the injector face may be due to the fact that the simulation is a planar view, whereas the experiment provides a line-of-sight view. The third mode is more complex in that the study element is in a region where oscillations in both pressure and velocity are present. Strong similarities can be seen nonetheless, with the heat release mode comprising four quadrants of alternating excess and deficit.

DMD analysis was also used to further explore the relationship between heat release and velocity. Figure 10 shows heat release, axial velocity and transverse velocity filtered at the primary chamber frequency with the mean value subtracted. The top row shows when the transverse velocity is the strongest. Interestingly, there appears to be two major transverse velocity regions with the primary one located just downstream of the injector elements. The bottom row shows when transverse velocity is the weakest. The relationship between transverse velocity and heat release can be understood when looking at the phase angle between the two, as shown in Figure 11. Heat release and transverse velocity are out of phase so when the transverse velocity is lowest, the heat release is the highest. Comparing the modes between the first and second rows in Figure 10 it appears that with the high transverse velocity, a swirling region is created and the heat release is perturbed. The heat release then detaches from the injectors once the transverse velocity has subsided and the swirling regions expand outward.

V. Conclusions

Hybrid RANS-LES simulations of a rectangular combustion chamber with forced transverse mode oscillations have been conducted. Companion experiments employ an array of injectors with the study injector element in the center and six driving injectors arranged linearly on either side of the study element. The driving injectors are tuned to sustain high amplitude combustion instabilities in the chamber. The simulations simplify the geometric configuration by replacing the driving injectors with an injection boundary condition and use an oscillating wall boundary condition to generate the transverse acoustic modes. By adjusting the amplitude of the wall velocity, the pressure amplitude is tuned to match the experimental values. A comparison of the pressure mode shapes show reasonable agreement of the between the computation and experiments. Power spectral density (PSD) analyses of the pressure signal at the wall demonstrate similar frequencies and amplitudes for the first three modes. The pressure waveforms at each port location show that the travelling compression wave qualitatively matches the experimental results although differences exist in the precise shape of the waveform.

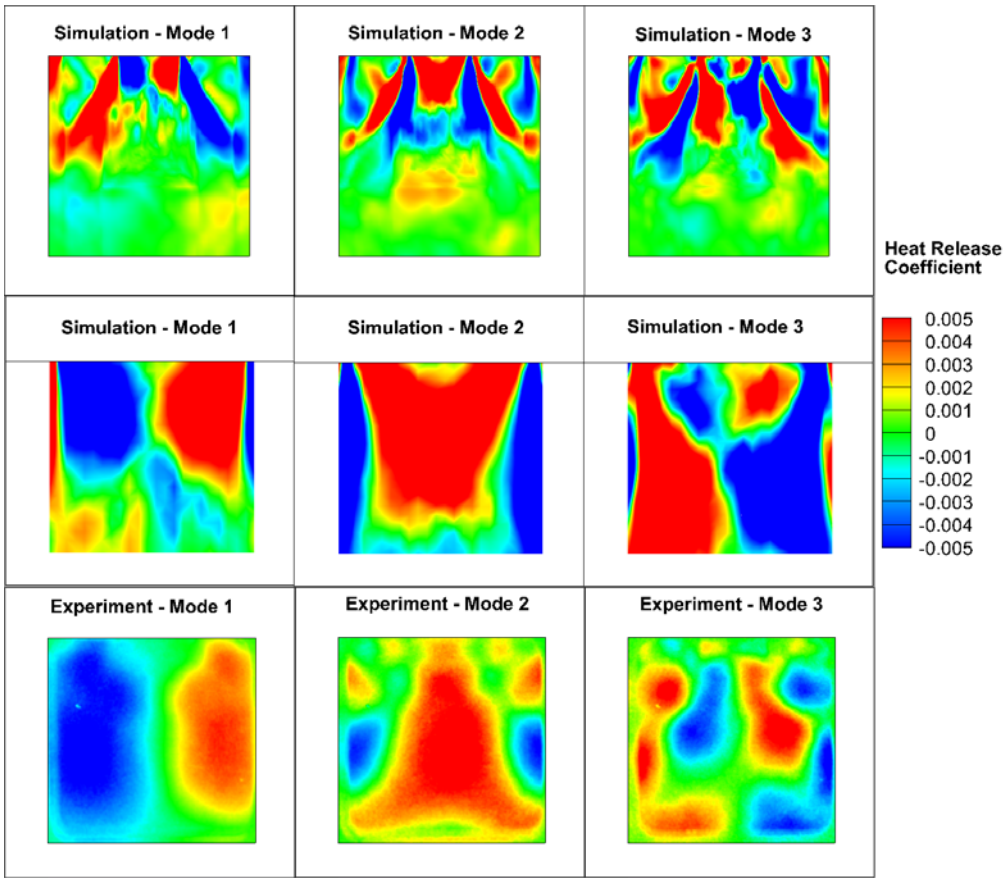

Figure 9: DMD comparison between the simulation (top row) and experiment (bottom row). The middle row is a zoomed in view of the top row.

A dynamic modal decomposition (DMD) technique is used to compare CH* chemiluminescence images from the experiment with the combustion heat release from the simulation. The resulting spatial modes are observed to be very similar, with some minor differences that could be attributed to limitations of the line-of-sight measurements. The DMD analysis is also applied to other the axial and transverse velocities showing that this technique is useful in isolating local phenomenon. Specifically, a strong reaction of combustion heat release to the transverse velocity is visible in the region downstream from the study element.

Overall, the results confirm that the simulations with the oscillating wall condition are able to replicate the experimental flowfield reasonably well. However, the procedure requires the tuning of the amplitude of the wall oscillations to match the experimental amplitudes. Future work will employ a more complete computational model that includes all seven injector elements so that the transverse modes are self-excited by the operation of the driving injectors.

Acknowledgments

The experimental work was funded by a Phase II SBIR Program funded by the Air Force Research Lab. The lead author was sponsored by a NASA Space Technology Research Fellowship. We would specifically like to thank BJ Austin of IN Space LLC for his help with this project, and Doug Talley of AFRL for his encouragement and support. We would also like to thank Kevin Tucker and Matt Casiano of NASA Marshall Space Flight Center.

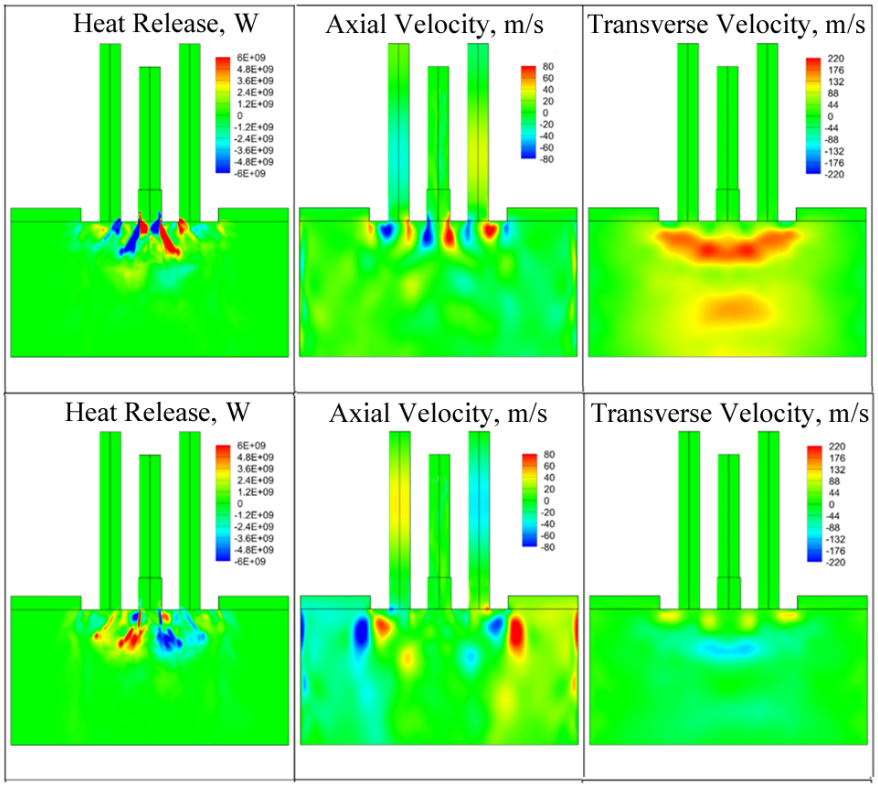

Figure 10: DMD analysis of heat release and velocity.

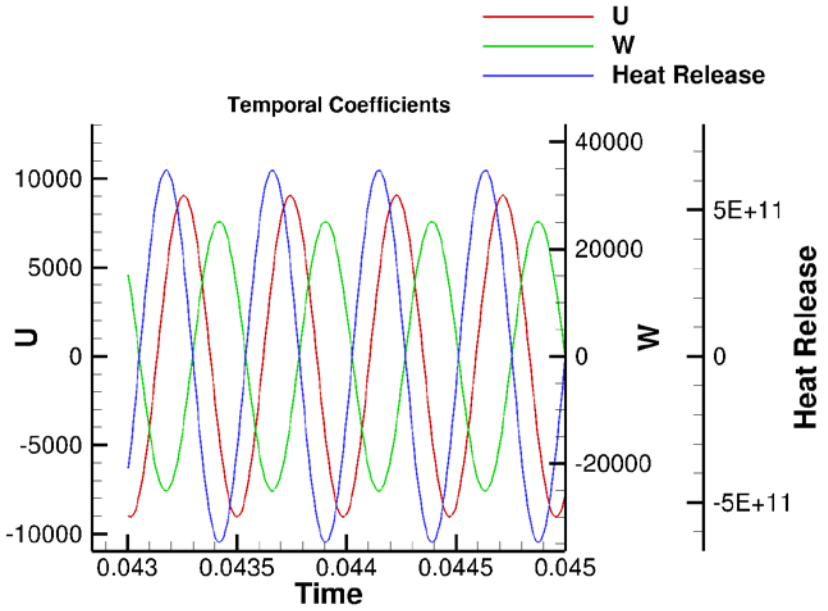

Figure 11: Temporal DMD analysis of mode 1

References

1. Harrje, D. T., and Reardon, F.H. (eds.), “Liquid Propellant Rocket Combustion Instability,” NASA SP-194, 1972
2. Yang, V., and Anderson, W. (eds.), Liquid Rocket Engine Combustion Instability, Vol. 169, Progress in Astronautics and Aeronautics, AIAA, Washington, D.C., 1995.
3. Hulka, J., “Scaling of Performance in Liquid Propellant Rocket Engine Combustion Devices,” AIAA 2008-5113.
4. Pomeroy, B., Lamont, W., Anderson, W., “Subscale Tool for Determining Transverse Combustion Response,” 45th JPC, AIAA 2009-5490.
5. Li, D., Xia, G., Sankaran, V., and Merkle, C., “Computational Framework for Complex Fluids Applications," 3rd International Conference on Computational Fluid Dynamics, Toronto, Canada, July 2004.
6. Xia, G., Sankaran, V., Li, D., and Merkle, C., “Modeling of Turbulent Mixing Layer Dynamics in Ultra-High Pressure Flows," 36th AIAA Fluid Dynamics Conference and Exhibit, San Francisco, CA, June 2006, AIAA Paper 2006-3729.
7. Lian, C., Xia, G., and Merkle, C., “Impact of Source Terms on Reliability of CFD Algorithms," The 19th AIAA Computational Fluid Dynamics, San Antonio, TX, June 2009.
8. Lian, C., Xia, G., and Merkle, C., “Solution-Limited Time Stepping to Enhance Reliablity in CFD Applications," Journal of Computational Physics, Vol. 228, 2009, pp. 4836-4857
9. Pomeroy, B., Nugent, N., Anderson, W., “Measuring Transverse Combustion Stability at Full Scale Frequencies in a Subscale Combustor”, 46th JPC, AIAA 2010-7146.
10. Ducruix, S., Rey, C., Candel, S., “A Method for the transverse modulation of reactive flows with application to combustion instability,” Combustion Theory and modeling , Vol. 9, February 2005, p. 5-22.
11. Westbrook, C., Dryer, F., “Simplified Reaction Mechanisms for the Oxidation of Hydrocarbon Fuels in Flames,” Combustion and Science Technology, 1981 Vol. 27, pp. 31 – 43.